https://doi.org/10.1016/j.applthermaleng.2017.04.108

Dependence of Flame Height of Internal Fire Whirl in a Vertical Shaft on Fuel Burning Rate in Pool Fire

W.K. Chow*
Department of Building Services Engineering
The Hong Kong Polytechnic University
Hong Kong, China

J.F. Dang and Y. Gao
College of Aerospace and Civil Engineering
Harbin Engineering University
Harbin, Heilongjiang, China

C.L. Chow
Department of Architecture and Civil Engineering
City University of Hong Kong
Hong Kong, China

*Corresponding author:
Fax: (852) 2765 7198; Tel: (852) 2766 5843
Email: beelize@polyu.edu.hk; bewkchow@polyu.edu.hk
Postal address: Department of Building Services Engineering, The Hong Kong Polytechnic University, Hunghom, Kowloon, Hong Kong.

Submitted: October 2016
Revised: March 2017

Abstract

An internal fire whirl (IFW) was generated by a pool fire in a vertical shaft with appropriate ventilation provision at the wall. The flame height of the IFW was found to increase with the burning rate of the pool fire. Semi-empirical formula for flame height in the IFW was studied analytically in this paper using reported experimental data from full-scale burning tests. Burgers vortex theory was applied for dynamic and thermodynamic corrections. From the experimental data, a rotating flame height coefficient was introduced to modify the empirical formula for the flame height in the IFW. Effects of thermal radiation and fuel vaporization were included to modify the calculation of the fuel burning rate.

Keywords: Fire whirl, Flame height, Rotating flame height coefficient, Fuel burning rate, Burgers vortex theory, Full-scale burning test

1. Introduction

Experimental studies reported that a fire burning in an enclosure such as a vertical shaft [1-4] or a small room [5-7] will give an internal fire whirl (IFW) under appropriate ventilation provision. The flame height and the burning rate of the pool fire inside a vertical shaft increased by several times of the same pool fire in open space. The burning time of the pool fire in an IFW was then reduced to only half of that of a free burning fire. Having a tall flame height would be much more hazardous as it might ignite adjacent combustibles and damage building walls, particularly those with fibre reinforced polymers in building retrofits.

Studying the flame height of an IFW is very important in fire hazard assessment of vertical shaft in tall buildings. Flame height will be studied analytically in this paper. IFW generated by burning a gasoline pool in a vertical shaft was reported before [8]. Part of the reported experimental data [8] will be used to develop an empirical formula relating the flame height of an IFW with the fuel burning rate in the pool. Results are then justified by comparing with simulation results using the computational fluid dynamics (CFD) software FLUENT [9].

In addition to numerical study, semi-empirical formula on flame height of the fire whirl was established. Experimental data is used to revise coefficients of the fire whirl height semi-empirical formula. More theoretical study will be discussed in future publications.

2. Flame Height of Fire Whirl

Variation of mass burning rate $\dot{m}''$ of fuel pool in free space with the pool diameter D was summarized by Chatris et al. [10]. $\dot{m}''$ changes with D when D is less than 2 m, varying from 0.055 kg/m^{2}s to 0.08 kg/m^{2}s. Earlier studies reported that $\dot{m}''$ does not change with D when D is larger than 2.0 m, but later modified the conclusion, stating that $\dot{m}''$ is constant only when D is larger than 3.0 m ([10]).

When the diameter of the fuel pool is larger than 1 m, the radiative heat of the liquid surface is 5/6 of the total surface radiation as reported by Shinotake et al. [11]. For D less than 1 m, especially when $0.3\text{m} < D < 0.6\text{m}$, the radiative heat of the liquid surface is 2/3 of the total surface radiation. Therefore, the effect of radiative heat transfer on mass burning rate of fuel $\dot{m}''$ at surface for 0.3 m < D < 0.6 m should be watched carefully.

From the findings of McCaffrey [12], Heskestad [13], Hasemi and Tokunaga [14] and Steward [15], the non-dimensional flame height L_f / D is directly proportional to $Q^{*2/5}$, where L_f and Q^* the flame height and a non-dimensional heat release parameter, respectively, for pool fire in free space.

The relationship between the flame height L_f of fire whirl (in m) and Q^* for an IFW is proposed to be modified in this paper by introducing a flame height factor X:

$$L_f = X \cdot Q^{*2/5} D \tag{1}$$

Q^* is given in terms of the heat release rate $\dot{Q}$ (in kW), density of ambient air ρ_0 (in kg/m^3), ambient temperature T_0 (in K), specific heat of air C_p (in kJ/kg-K), and acceleration due to gravity g (in m/s^2) by [12]:

$$Q^* = \frac{\dot{Q}}{\rho_0 T_0 C_p \sqrt{gD} D^2} \tag{2}$$

In the fuel burning process, the relationship between heat release rate $\dot{Q}_c$, fuel burning rate $\dot{m}$ and heat combustion of fuel H_c is

$$\dot{Q} = \dot{m} \cdot H_c \tag{3}$$

The fuel burning rate $\dot{m}$ of a pool fire under free burning condition is given in terms of the

maximum mass burning rate of fuel per unit surface area $\dot{m}''_{\max}$, (in kg/m^{2}s), surface area of pool fire A, (in m^2), where $A = \frac{\pi D^2}{4}$, and an empirical constant $k\beta$:

$$\dot{m} = \dot{m}''_{\max}(1 - e^{-k\beta D})A \qquad (4)$$

Actually, k and β are constants, giving a constant value of $k\beta$. In this place, $k\beta$ is taken as one constant.

Putting Eqs. (2) to (4) into Eq. (1),

$$L_f = X\left(\frac{\dot{Q}}{\rho_0 T_0 C_p \sqrt{gD}D^2}\right)^{2/5} \cdot D$$

or

$$L_f = X\left(\frac{\dot{m}''_{\max}(1 - e^{-k\beta D})A \cdot H_c}{\rho_0 T_0 C_p \sqrt{gD}D^2}\right)^{2/5} \cdot D \qquad (5)$$

Note that Eq. (5) is an empirical formula for the flame height under free burning condition. Thus it needs modification for adaptation to the case of internal fire whirl.

Two points in these equations are worth noticing in the modification:

Firstly, the flame height factor *X* in Eq. (1) was suggested by Steward [15] to be 3.3, based on experimental studies on pool fire in free space. In studying L_f for a fire whirl, the tangential velocity u_θ should be considered with the effect of the axial vorticity Ω_z included in calculating the flame height. As observed from the photographs taken in generating fire whirl, the flame surface of fire whirl rotated vigorously along the axis. The folding of flame surface was obvious. The rotation speed caused an increase of the flame height of the fire whirl and reduction of the radius of the pool fire surface. The flame height factor *X* in Eq. (1) was originally introduced for pool fire in free space where only buoyancy was considered. Thus the flame height factor *X* has to be modified in calculating flame height of fire whirl where the hydrodynamic condition is much more complicated.

From previous experiments by Chow [8], the flame height factor *X* is greater than 3.3, and could be up to 3.59. Although the experimental results in [8] indicated that rotational flow

would increase X, a constant flame height factor cannot show the effect of rotational flow on fire whirl with different air entrainments and fuel vaporization. Therefore, dynamic correction to the flame height factor X should be made. In this study on IFW, the flame height factor X is re-named as the rotating flame height coefficient X_{fw} in order to differentiate it from the "flame height factor X " commonly used for fire in free space and to emphasize its applicability in IFW.

Secondly, Eq. (5) can be conveniently expressed in terms of a thermal parameter h_p (which depends on the pool fire characteristics), and a physical parameter p_p (which depends on the physical properties of ambient air), and X_{fw}:

$$L_f = X_{fw} h_p p_p \tag{6}$$

with

$$\begin{cases} h_p = \left[\dot{m}''_{\max}(1-e^{-k\beta D})\cdot A\cdot H_c\right]^{2/5} & \text{(6a)} \\ p_p = (\rho_0 T_0 C_p)^{-2/5}\cdot g^{-1/5} & \text{(6b)} \end{cases}$$

For a fire whirl, the physical parameter p_p in Eq. (6) is a constant as it is not related to the fire pool. Therefore, correction is not required for p_p. As h_p is related to the fuel burning rate of a free burning pool fire, correction is needed for fire whirl with different fuel burning rate.

In establishing the semi-empirical formula for the flame height of the fire whirl, the vortices were introduced. Theories of Burgers and Sullivan vortices were based on the thermal buoyancy. FLUENT CFD simulations with FLUENT were also based on the thermal buoyancy without thermal radiative feedback from the gas phase to support evaporation. The semi-empirical formula was derived from experimental results in reference 8 as summarized in Table 1. In the experiment, the amount of fuel, burning area and burning time were measured. The burning rate of the pool fire under steady state depends on heat radiation and the burning surface of the revolving turbulent flow characteristics. As the semi-empirical constant was deduced from experiment, thermal radiative feedback effects were included. In numerical calculations, the flow state of Arrhenius law and turbulent eddy dissipation concept model were used to study the fuel surface temperature on the chemical reaction rate. Thermal radiation was then absorbed in the fuel oil liquid surface, the temperature increased and vaporization took place.

3. Elaboration of the Rotating Flame Height Coefficient X_{fw} for IFW

Experiments on IFW were reported [8] in a vertical shaft rig of 9 m tall as shown in Fig. 1. When a gap of width 0.33 m was provided, an IFW was induced under a gasoline pool fire of diameter 0.43 m. Some photographs for 2 tests SW-20 and SW-21 taken in the experiment are shown in Fig. 2. Five tests SW-A, SW-18, SW-20, SW-21 and SW-22 are taken out for this study. Except pool fire diameters, the testing conditions were all the same for the SW-A, SW-18, SW-20, SW-21 and SW-22 on the vertical shaft geometry and the liquid fuel. The dimensions of the shaft are shown in Fig. 1. Thermocouple trees as in Fig. 1c were put at positions M (centre) and C (corner) as in Fig. 1. Different fire pool diameters would give different fuel consumption rates. Test information on fitting empirical equation (or tests SW-A, SW-18, SW20, SW-21 and SW-22) is shown in Table 1.

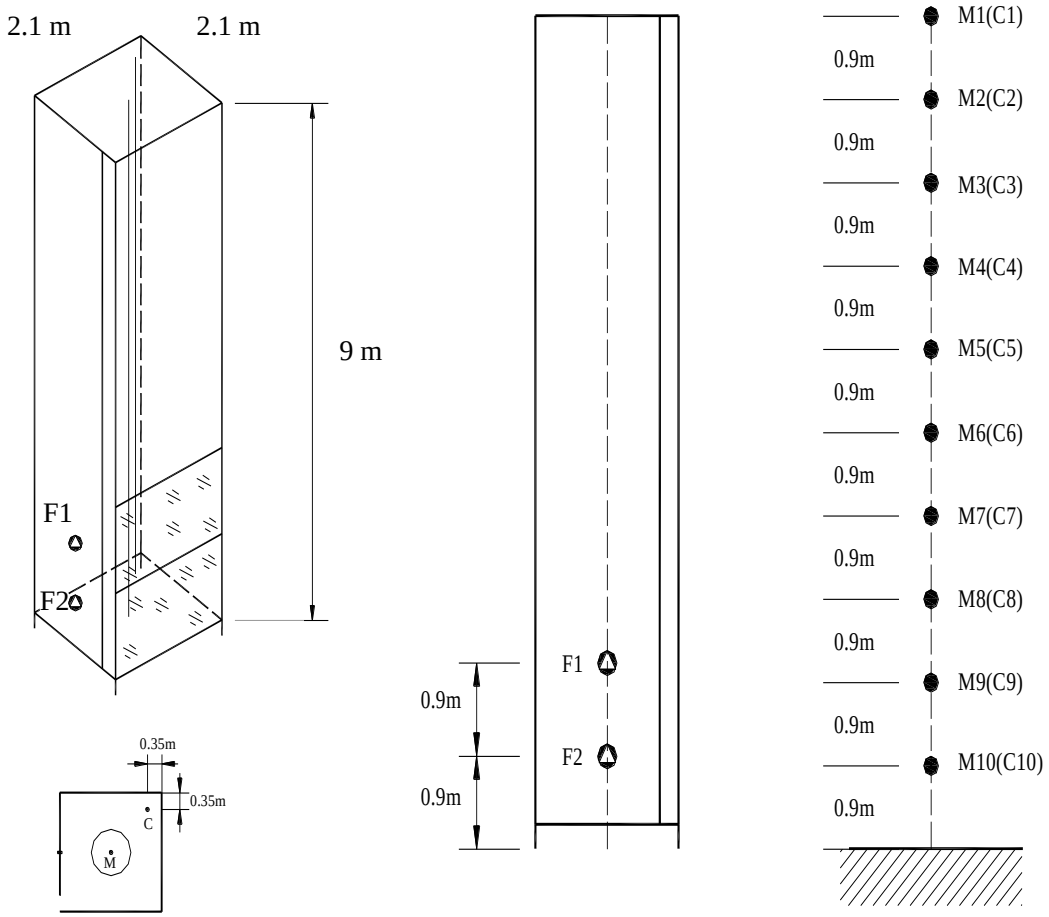

(a) Main dimensions (b) Position of heat flux meters (c) Position of thermocouples

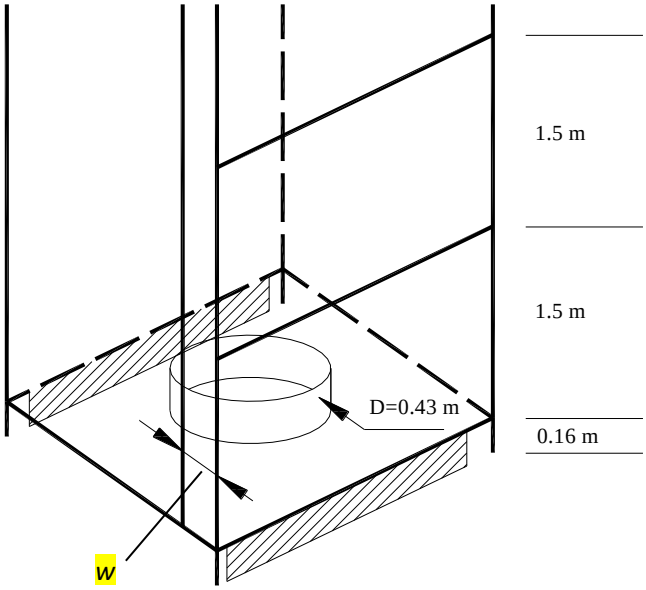

(d) Details above the pool fire

Fig. 1: Experiment rig

(a) SW-20

(b) SW-21 at bottom

(c) SW-21 at middle

Fig. 2: Observed swirling of the internal fire whirls

Table 1: Experimental results reported by Chow et al. [2011]

Test	$\dot{m}''$ （kg/m^{2}s）	$\dot{Q}_c$ （kW）	Experimental flame height $\overline{L}$ (m)
SW-A	0.0327	285	1.3
SW-18	0.073	323	1.4
SW-20	0.153	677	2.8
SW-21	0.139	617	2.6
SW-22	0.152	679	2.8

As reported by Hayashi et al. [16] on flame base under four conditions for a pool fire in free space, there is no rotational flow induced. As observed, the flame surface of a free burning pool fire is smooth, very different from the rough flame surface of IFW. The flame surface of an IFW has some folds caused by the upward cylindrical burning movement. This upward spiral movement causes the flame surface of the fire whirl to extend and increases the fuel burning rate. Therefore, it is not appropriate to calculate the flame height of fire whirl by using the flame height equation derived for free burning fire, where a constant flame height factor X is included. Constant flame height factor cannot take into account the flow and burning characteristics of fire whirl. Therefore, it is crucial to replace X by a newly defined rotating flame height coefficient X_{fw} in dealing with IFW.

Vortex theory was included in combustion dynamics to study rotating flow and burning phenomenon of fire whirl. For example, Hayashi et al. [16] conducted experiment to study the effect of vortex structure on the characteristics of fire whirl. The flame swirling angle a was determined near the liquid fuel to calculate the flame height, and the flame height of fire whirl can be fitted by a parabolic relationship:

$$\begin{cases} L_f = a_L \cdot (r + H/2)^{1/2} \\ L_f = a_R \cdot (r - H/2)^{1/2} \end{cases} \tag{7}$$

In Eq. (7), a_L, a_R are the flame angles near the liquid fuel, H is the height of the experiment rig of the fire whirl; r is the radius of the fire whirl. As pointed out [8], the distribution of radial velocity near the liquid fuel has a great influence on the flame height.

Klimenko and Williams [17] carried out analytical study on the effect of strong vortex structure on fire whirl flame height. On top of the original flow basis, vortex speed compensation was introduced to predict the effect of strong rotational flow. Klimenko and Williams [17] showed that the flame height equation is given by:

$$L_f = r_0 \frac{\mathrm{Pe}}{4\alpha_{eff} Z_{st}} \tag{8}$$

In Eq. (8), r_0 is the radius of fire whirl, Pe is Peclet number, for Burgers vortex, $\alpha_{eff} = 2.0$, Z_{st} is the corresponding boundary condition of the average flame height of fire whirl.

Chuah and Kushida [18] also introduced vortex theory to the prediction of flame height and

flame shape of small fire whirl with results similar to using Sullivan Vortex theory. Note that an ideal flow model will be introduced when using the Burgers vortex theory [19]. The equation for the flame height obtained by Chuah and Kushida [18] is given by:

$$L_f = \frac{Q}{4\pi D_0 \ln(1+1/S)}\left(\frac{T_0}{T_f}\right)^{n-1} \tag{9}$$

In Eq. (9), T_0 is the ambient temperature, T_f is the flame temperature, S is the stoichiometric volume air-fuel ratio, D_0 is the ambient diffusivity coefficient, n is the diffusivity exponential coefficient, and Q is the mass burning rate.

It is observed from Fig. 2 that in the swirling flow streamlines of the fire whirl flame surface, the flow velocity can be divided into circumferential velocity u_θ and axial velocity u_z. The centripetal force and axial vortex Ω_z caused by u_θ would increase the surrounding air entrainment at the flame surface. u_z causes the flame to develop axially. Both of them together would create an effect to increase the flame height. Introducing Burgers vortex theory [19], the velocity distribution at the vortex core for $0 \le r < c$ is given by:

$$\begin{cases} u_r = -\dfrac{2\upsilon_f}{f^2} r \\ u_\theta = \dfrac{\Gamma}{r}\left(1 - e^{-\frac{r^2}{f^2}}\right) \\ u_z = \dfrac{4\upsilon_f}{f^2} z + u_{z0} \end{cases} \tag{10}$$

In Eq. (10), Γ is the velocity circulation of u_θ; f is the flame radius, r is the radial coordinate, υ_f is the kinematic viscosity of the flame, z is the axial coordinate, u_{z0} is the axial velocity when $z = 0$, and c is the radius of the vortex core. The axial vortex Ω_z is governed by the following equation:

$$\Omega_z = \frac{1}{r}\frac{\partial(ru_\theta)}{\partial r} - \frac{1}{r}\frac{\partial u_r}{\partial \theta} \tag{11}$$

Axial velocity u_z and axial vortex enhance the development of the flame of fire whirl. However, gravitational acceleration hinders the development of fire whirl. Therefore, the rotating flame height coefficient of fire whirl X_{fw} of L_f in Eq. (6) is proposed to be

expressible as:

$$X_{fw} = \frac{u_z \Omega_z}{g} \tag{12}$$

Using the dimensions given in parentheses, $u_z\left(m/s\right)$, $\Omega_z\left(s^{-1}\right)$, $g\left(m/s^2\right)$, dimensional analysis of the rotating flame height coefficient shows that it is dimensionless :

$$X_{fw} = \frac{u_z \Omega_z}{g} = \frac{\left(m/s\right)\left(s^{-1}\right)}{m/s^2} = 1 \tag{13}$$

Thus the rotating flame height coefficient X_{fw} is a dimensionless coefficient that incorporates the effect of the flow burning characteristics of fire whirl.

Chigier and Bedr [20] proposed a Swirl Number S_{CB} defined as:

$$S_{CB} = \frac{G_{tg}}{RG_{ax}} = \frac{\int_0^R u_\theta u_z r^2 dr}{R\int_0^R u_z{}^2 r dr} \tag{14}$$

In Eq. (14), G_{tg} is the tangential axis momentum flux, G_{ax} is the axial momentum flux, R is the rotating outer radius. At the same time, it can also be defined as:

$$S_m = \frac{J_{tg}}{J_{ax}} = \frac{\int_0^R u_\theta u_z r dr}{\int_0^R u_z u_z r dr} \tag{15}$$

In Eq. (15), J_{tg} is the circumferential velocity momentum, and J_{ax} is the axial velocity momentum. Both S_{CB} and S_m only take into account the effect of circumferential velocity on rotating flow. It can be observed that the definition of Swirl Number does not take the obstruction effect of gravitational acceleration g on the flow into consideration. In comparison, the newly defined rotating flame height coefficient X_{fw} is more meaningful in dealing with the flame height of fire whirl.

Suppose the radius of vortex core and that of the flame are the same, $f = c$. At the flame surface, $f = c = r$. Substituting it into Eq. (10):

$$\left.\begin{aligned} u_r &= -\frac{2\upsilon_f}{r} \\ u_\theta &= \frac{\Gamma_0}{r}\left(1-e^{-1}\right) \\ u_z &= \frac{4\upsilon_f}{r^2}z + u_{z0} \end{aligned}\right\} \quad f = c = r \tag{16}$$

Suppose Γ is a constant, and take the velocity circulation at z = 0 m to be Γ_0. Then $\Omega_z = \frac{1}{r}\frac{\partial\left(ru_\theta\right)}{\partial r} - \frac{1}{r}\frac{\partial u_r}{\partial\theta} = \frac{\Gamma_0}{r^2}\mathrm{e}^{-1}$, and the rotating flame height coefficient is given by:

$$X_{fw} = \frac{u_z\Omega_z}{g} = \frac{\Gamma_0 e^{-1}\left(4\upsilon_f z + r^2 u_{z0}\right)}{r^4 g} \tag{17}$$

X_{fw} is a global factor for the fire whirl, depending on z. At different heights of the fire whirl, the combustion and entrainment conditions are different, giving different X_{fw} at different heights, i.e. X_{fw} depends on z. Therefore, X_{fw} is plotted as a function of z (r fixed) and r (z fixed) in Fig. 3, with Γ_0 = 1.57 m^2/s, υ_f = 0.0003 m^2/s, u_{z0} = 0.27 m/s. From Fig. 3(a), X_{fw} increases as z increases, the initial value is determined by the velocity circulation Γ_0 just above the oil pool. It can be observed that although X_{fw} increases linearly as z, the magnitude of increment is limited, which is from 0.38 to 0.51 within the whole flame height range. Hence, the average value for X_{fw} can be taken to be 0.45.

In Fig. 3(b), by taking different cross-section at different flame height, the variation of X_{fw} with respect to flame radius r at a specified height is plotted. It can be observed that, as the flame radius r increases, X_{fw} decays exponentially. In the range of 0.1 m > r > 0 m, X_{fw} decreases rapidly. For r > 0.3 m, X_{fw} approaches 0. However, for certain value of r, the magnitude change of X_{fw} with respect to flame height z is the greatest for z = 2.70 m, then z = 0.16 m, z = 0.32 m and z = 0.64 m, the lowest value is at z = 1.28 m.

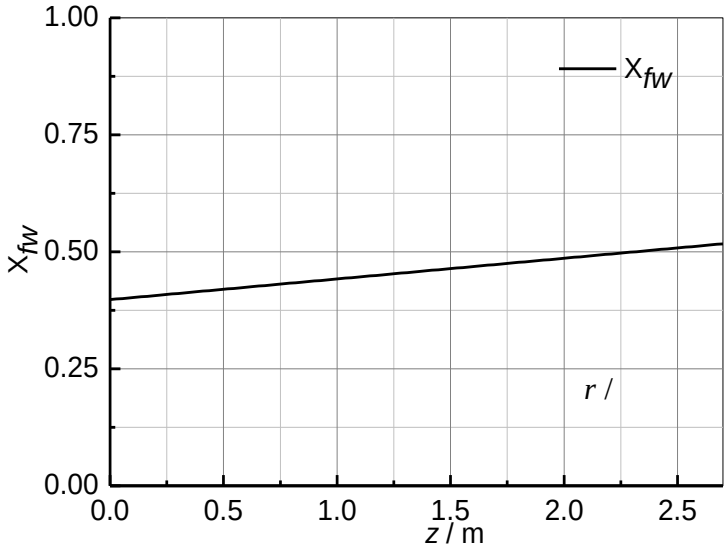

(a) X_{fw} as a function of z

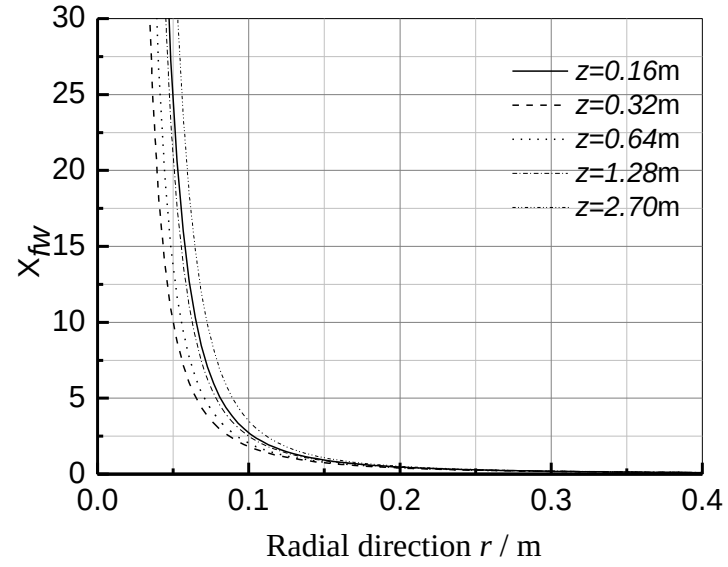

(b) X_{fw} as a function of r

Fig. 3: Variation of X_{fw} with z and r ($\Gamma_0 = 1.57\,\mathrm{m^2/s}$, $\upsilon_f = 0.0003\,\mathrm{m^2/s}$, $u_{z0} = 0.27\,\mathrm{m/s}$)

4. Correction to the Thermal Parameter h_p

An important element of the thermal parameter h_p is the knowledge of the mass consumption rate of fuel per unit area $\dot{m}''$ of IFW during steady burning. For hydrocarbon liquid fuel, it was pointed out that the determination of $\dot{m}''$ is crucial. Blinov and Khudiakov [21] and Hottel [22] have suggested an empirical formula for $\dot{m}''$ in a free burning fire:

$$\dot{m}'' = \dot{m}''_{\max}(1 - e^{-k\beta D}) \tag{18}$$

Regarding fire whirl, different empirical constants were suggested from experimental data. Lei et al. [23] determined $k\beta$ from their heptane fuel fire whirl experiment. Also focusing on heptanes fuel fire whirl, Tarifa [24], Kung and Stavrianidis [25], and Klassen and Gore [26] suggested the empirical formula to be:

$$\dot{m}'' = 0.072(1 - e^{-2.49\mathrm{D}}) \tag{18a}$$

The conclusion drawn from the above experiments is different from that summarized by Chatris et al. [10] on the effect of oil pool radius on $\dot{m}''$. In addition, there is difference in the reported average value of $\dot{m}''$. The average value of $\dot{m}''$ was found to be ranging from 0.055 kg/m^{2}s to 0.08 kg/m^{2}s for a freely burning pool fire by Chatris et al. [10], while Lei et al. [23] reported that the average value of $\dot{m}''$ ranged from 0.075 kg/m^{2}s to 0.088 kg/m^{2}s. This shows that the value of $\dot{m}''$ in fire whirl is larger than that in a free burning fire even for an oil pool of small diameter D. Thus, fire whirl poses a significant enhancement effect on the fuel burning rate of the oil pool.

In order to further investigate the relationship between the flame height of fire whirl and the fuel burning rate, earlier experimental data [8] obtained from gasoline fuel fire whirl tests as in Fig. 1 were used, with results summarized in Table 1. Photographs of the fire whirl under stable burning condition in the 4 tests are shown in Fig. 4. In the test, the height of the oil pool H was 0.15 m. There was no fire whirl generated in test SW-A and SW-18 for free burning fire while for tests SW-21 and SW-22, there were stable fire whirl generated. The photographs show clear folds on the flame surface which is moving upwards cylindrically.

From the test results shown in Table 1, it can be observed that the flame height of fire whirl is 2 times the flame height of a free burning fire. Also, the fuel consumption rate per unit surface area $\dot{m}''$ reached 0.139 kg/m^{2}s to 0.152 kg/m^{2}s. This value is much higher than the corresponding value in a free burning fire and is also higher than the fuel consumption rate of the heptanes fire whirl conducted by Lei et al. [23]. Therefore, it is not appropriate to deduce

the flame consumption rate of fire whirl based on the equation of fuel consumption for free burning fire. The fuel consumption rate of fire whirl will be obtained based on the reaction mechanism and this rate will then be used for modifying the empirical equation on flame height in IFW.

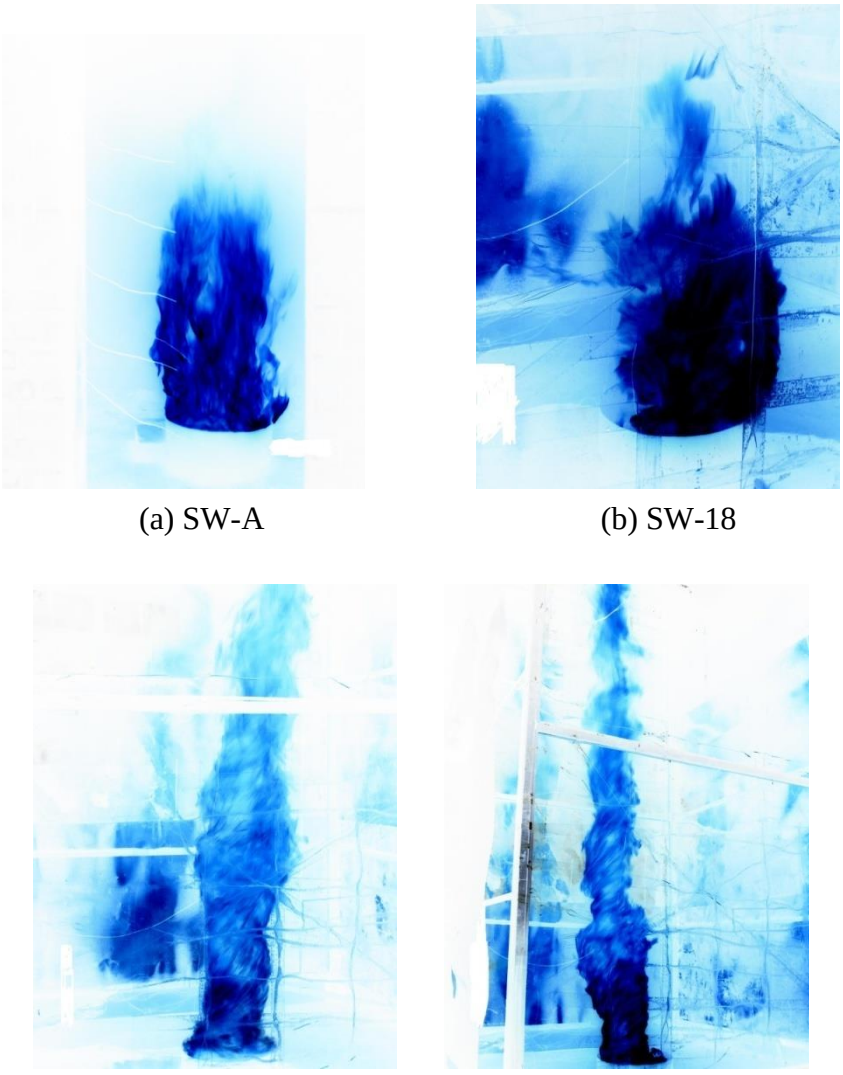

(a) SW-A (b) SW-18

(c) SW-21 (d) SW-22

Fig. 4: Burning characteristics in the four different experiments

It was observed from the tests [8] that in the fire whirl, vaporization occurred both at the liquid fuel surface and the contact surface between the oil and the pool wall. Thus, there was vaporization occurring inside the oil pool. Ignoring the contact area between the liquid and the oil pool side wall, the area of vaporization A has been increased from liquid surface of free burning condition to 2A when there is an IFW. The effective vaporization area was doubled. This is consistent with the earlier result [8] that the fuel burning rate was also increased from $0.073 kg/m^2 s$ in test SW-18 (free burning) to $0.146 kg/m^2 s$, which is the

average value of test SW-21 and SW-22 (IFW),with doubling of the fuel burning rate. Hence, this explains why $\dot{m}''$ obtained in fire whirl tests SW-21 and SW-22 is much higher than that of the value obtained in the heptanes fire whirl experiments by Lei el al. [23].

Taking into account of the observation that the oil pool wall significantly contributes to $\dot{m}''$, the equation of fuel burning rate is reformulated as below:

$$\dot{m}'' = \frac{1}{L_v}\left\{\frac{h_c}{c_p}\left(\frac{\xi}{e^{\xi}-1}\right)\left[\Delta H_c(Y_{o_2}/\gamma)(1-\chi_r) - c_p(T_v - T_a)\right] - \frac{2k_w}{\delta}(T_v - T_w) + \dot{Q}_{f\cdot rad}(1-r_s) - \varepsilon\sigma T_v^{\,4}\right\} \tag{19}$$

In Eq. (19), L_v is the specific latent heat of gasification, c_p is the specific heat capacity at constant pressure, $\xi = \frac{\dot{m}'' c_p}{h_c}$, h_c is the convective heat transfer coefficient, ΔH_c is the efficiency of heat release of burning, Y_{o_2} is the mass fraction of oxygen, γ is the stoichiometric mass ratio, χ_r is the radiative heat transfer ratio, T_v is the vaporization temperature, T_a is the ambient temperature, T_w is the oil pool wall surface temperature to be determined by experiment, k_w is the thermal conductivity of the oil pool wall, δ is the oil pool wall thickness, $\dot{Q}_{f\cdot rad}$ is the heat transmitted to oil surface through radiation, r_s is the radiation reflectance, $\varepsilon = 1 - e^{-k\beta D}$, and σ is the Stefan-Boltzmann constant.

On the right side of the equation, the first item represents the convection effect of the burning surface coming from combustion theory. The second item is surface heat absorption rate at temperature *T*. The third item is the incoming heat of the steel oil plate after heating. The fourth item is the net radiative heat transfer from the flame to the pool surface. The fifth item is the surface radiative heat loss.

In Eq. (19), $\xi = \frac{\dot{m}'' c_p}{h_c}$ consists of the unknown quantity $\dot{m}''$. Since the unknown $\dot{m}''$ appears on both sides of Eq. (19) and also as an exponent, numerical iteration is needed for solving the equation. Note that Eq. (19) is an implicit equation with solutions determined from numerical iteration method. T_w was determined form experimental data.

The correction to the thermal parameter h_p is completed after determining $\dot{m}''$. The total heat release rate of fuel $\dot{Q}$ is given by:

$$\dot{Q} = \dot{m}'' \cdot A \cdot H_c \tag{20}$$

A semi-empirical relation between the fire whirl flame height and the fuel burning rate of an

IFW at the stage with a stable swirling motion was studied in this paper. Modifications of P_p and h_p are proposed with Eq. (19) being the correction to the thermal parameter h_p. Once $\dot{m}''$ is fitted, the semi-empirical relation between the fire whirl flame height and the fuel burning rate can be developed.

5. Correction to Flame Height

After introducing X_{fw} and correcting h_p, the flame height equation of an IFW will be derived in this section. Writing Eq. (6) for the flame height in IFW in full,

$$L_f = X_{fw} \underbrace{\left[\dot{m}'' \cdot A \cdot H_c\right]^{2/5}}_{h_p} \cdot \underbrace{(\rho_0 T_0 C_p)^{-2/5}}_{p_p} \cdot g^{-1/5} \tag{21}$$

In addition to the introduction of a new rotating flame height coefficient X_{fw} and correction to h_p by considering oil vaporization at pool wall in the theoretical analysis of L_f, further modification is needed to take care of the boundary and initial conditions in the IFW test. This is achieved via introducing a coefficient α in Eq. (21), which now becomes:

$$L_f = \alpha X_{fw} \underbrace{\left[\dot{m}'' \cdot A \cdot H_c\right]^{2/5}}_{hp} \cdot \underbrace{(\rho_0 T_0 C_p)^{-2/5}}_{p_p} \cdot g^{-1/5} \tag{22}$$

In Eq. (22), X_{fw} is determined by Eq. (17), $\dot{m}''$ is determined by Eq. (19), and α is used to modify the relationship between L_f and $\dot{m}''$ based on the boundary and initial conditions of the test. L_f above is now expressed in terms of a thermal parameter h_p (which depends on the pool fire characteristics), and a physical parameter p_p (which depends on the physical properties of ambient air).

In the analysis of both X_{fw} and $\dot{m}''$, the effects of the boundary and initial conditions have not been taken into account. The effects of boundary condition on the flame characteristics can be observed from the photographs of tests SW-21 and SW-22 with swirling; and another test SW-23 without generating a fire whirl in Fig. 5. The boundary conditions of these 3 tests SW-21, SW-22 and SW-23 were different. Tests SW-21 and SW-22 had gap widths 0.33 m and 0.44 m respectively. Test SW-22 had no guard plate at the bottom of the vertical shaft. Therefore the test results are different. Stable fire whirl was formed in test SW-21 and SW-22 but their flame heights were different. The flame height for fire whirl in test SW-22 was higher than that in SW-21 (see Table 1). There was no fire whirl formed in test SW-23. According to various results reported in the literature, the characteristics of both natural fire whirl and enforced burning fire whirl are affected by boundary conditions [23,27,28].

It can be concluded from the observation above that different boundary and initial conditions of the test will give different results. Therefore Eq. (22) needs further modification to cater

for the effect caused by the boundary and initial conditions, via the introduction of a coefficient α. It is necessary in the future to conduct research on the explicit dependence of α on the boundary and initial conditions, to yield more accurate results for the fire whirl flame height.

(a) SW-21 (b) SW-22 (c) SW-23

Fig. 5: Flame heights in different experiments

6. Numerical Studies

Numerical simulation with CFD was carried out to justify the Burgers vortex theory used in deriving L_f and the thermodynamic correction focused on $\dot{m}''$. Since structured mesh has good convergence and data recovery ability, hexahedral structured mesh was used for the computing domain and the number of mesh was 400,000. Fig. 6 shows the mesh of the computing domain which was based on the experimental setup shown in Fig. 1. All the dimensions were based on the experimental data [8,23,27,28] in order to simulate the scenario of the experiment.

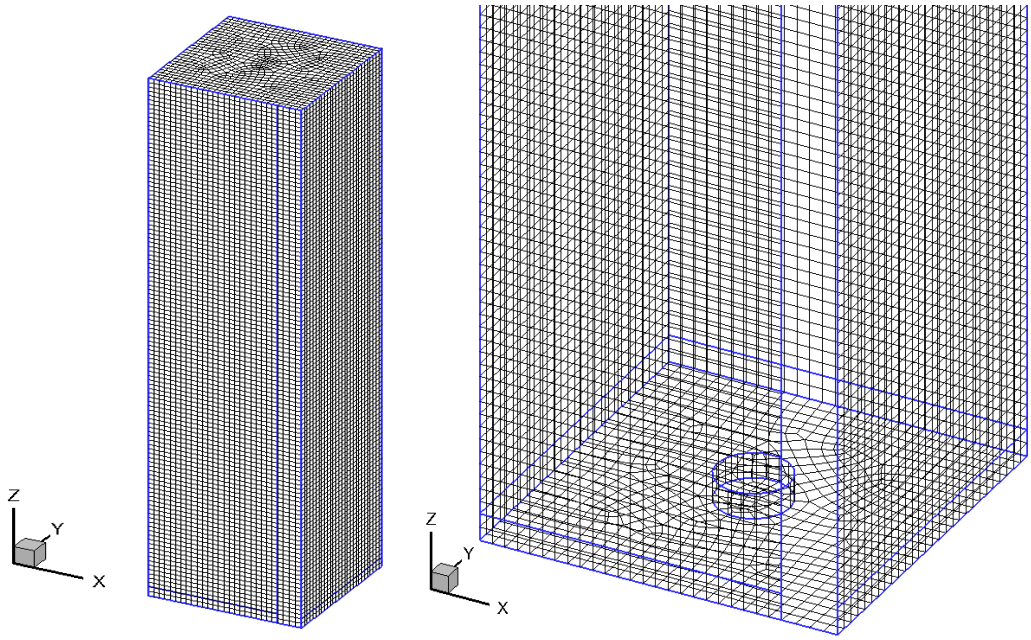

(a)Mesh of whole space (b) Mesh of the lower part

Fig. 6: Computing domain

Commercial software ANSYS FLUENT 13.0 [9] was used in the simulation. The boundary condition was set in the simulation as follows. Considering the requirement of free burning fire whirl by the software, the air intake pressure was set to be ambient pressure without including rotational flow. The fuel value used is the average test value $\overline{\dot{m}''} = 0.146\, kg/m^2 s$ of SW-20 and SW-21. As for the turbulence model, realizable $k-\varepsilon$ turbulence model with standard wall function was used. For chemical reaction, the eddy dissipation concept model was used.

In the calculation, gasoline used in the experiment was taken as C_8H_{18} with heat of combustion H_c of 44800 kJ/kg. Only the following chemical reaction was considered:

$$C_8H_{18} + 12.5O_2 \rightarrow 8CO_2 + 9H_2O \quad (23)$$

Fig. 7 shows the flame surface and streamline at 1000 K. It can be clearly observed that, at 1000 K the cylindrical streamline moving upward was surrounded by the outer part of the flame surface. The flame height was about 2 m to 3 m. The closer to the bottom of the flame surface, the more pronounced was the rotational characteristics of the streamline. Along the upward direction of flame movement, the angle of streamline rotation gradually increased. This matches with the conclusion drawn from the photographs in Fig. 2. At 1 m above the flame surface, the streamline rotation stopped. This means that the rotation of the flame surface caused the surrounding air to rotate as well. Hence, it would entrain more non-reacted air and enhance the burning of the fuel. This explains why the burning time of fire whirl is half of that of a free burning fire.

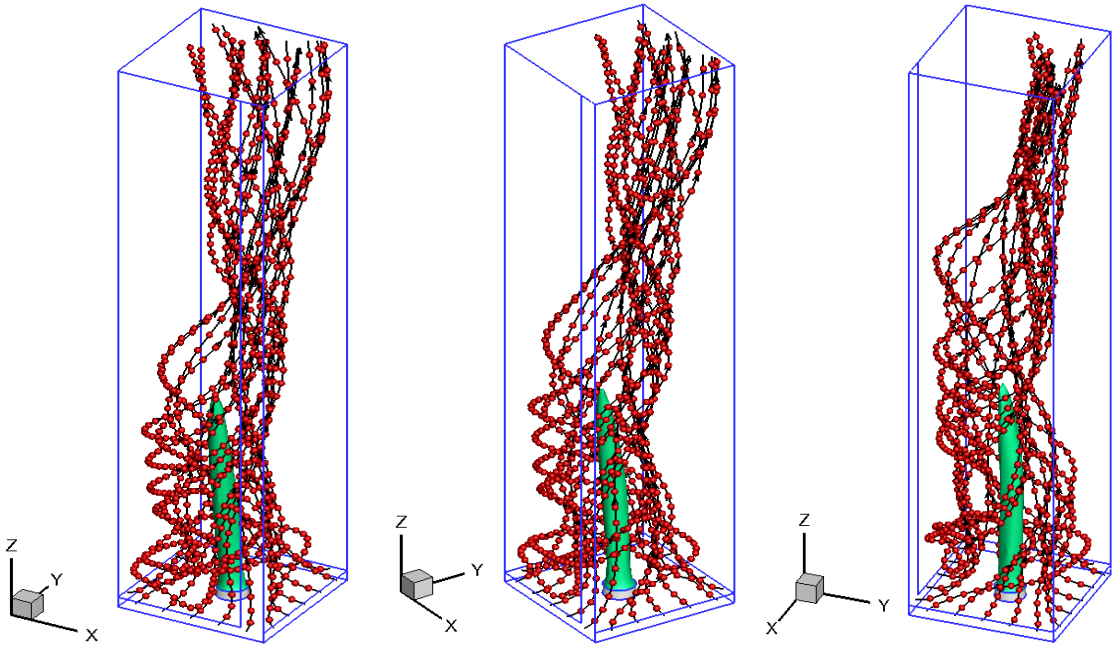

(a) View-a (b) View-b (c) View-c

Fig. 7: Three views of flame surface and streamlines

Fig. 8 shows the simulated dependence of the temperature and fuel mass fraction on height, where the data refer to the values along the axis of the oil pool. Taking 1000 K as the temperature of the top of the flame, it can be seen that the flame height was about 2.5 m to 2.6 m. This is consistent with the average flame height of 2.7 m in tests SW-20 and SW-21. In addition, the fuel mass fraction was equal to 0 at that point of flame height. This means that all the fuel at that point had completely reacted, which further justified the flame height calculated.

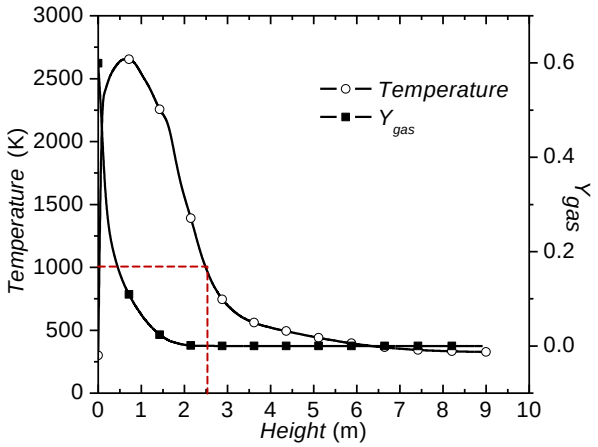

Fig. 8: Dependence of flame temperature and Y_{gas} on height

For experiments in this paper, the widths of the vertical and bottom gaps of the shaft model and the fire pool diameter can be adjusted. A fire whirl was only generated when there was an appropriate vertical gap width. With a fire whirl, the pool fire is similar to free burning. Further, before generating the swirling motion, the pool fire is also similar to free burning [29]. Note that 1000 K is not for justifying the flame height, but used as the isometric surface to observe the vortices flow in the fire core. It also explains why the Burgers and Sullivan vortices theories are used.

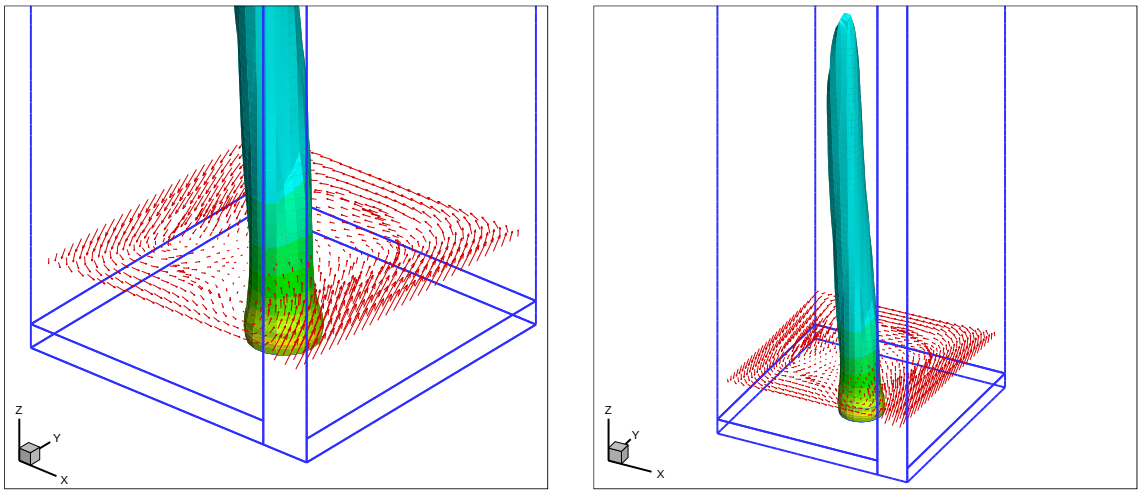

3 (a) 13 (b)

Fig. 9: Two views of flame temperature and velocity vectors in plane at $z = 0.3$

Fig. 9 shows the velocity vectors at the cross-section above the oil pool. It can be observed that the whole flow field surrounding the flame surface had a very distinct rotational characteristic. The center of rotation and the flame surface coincided with each other. Near

the side opening, the speed of rotation was faster than at other locations. This shows that the air entrainment of fire whirl was stronger near the side opening.

Based on the result and taking the average value $\overline{\dot{m}''}$ of 0.146 kg/m^{2}s as the calculated fuel mass flow for tests SW-20 and SW-21, the calculated flame height illustrated that the fuel consumption rate matched with the experimental results. The corrections suggested in above were thus justified. Further, the assumption that the increase in vaporization area caused by boiling in the oil pool of the fire whirl experiment is reasonable.

7. Conclusions

The following conclusions can be drawn from the study:

(1) Dynamic and thermodynamic corrections were made on the current flame height equation, and a semi-empirical formula (Eq. (22)) for flame height L_f of IFW was obtained, where X_{fw} is determined by Eq. (17), $\dot{m}''$ is determined by Eq. (19). A coefficient α was used to take care of the effect of the boundary and initial conditions of the experiment.

(2) Boiling of liquid fuel with combustion was observed in the oil pool during the evolution of fire whirl. Boiling with combustion would increase the area of vaporization, which is the sum of the area of free surface and bottom of oil pool. Thus, this also leads to the increase of unit area fuel consumption rate $\dot{m}''$ would then be increased to over twice of that in free burning condition. This phenomenon is also verified from calculation. The calculated flame height matches with the experiment result. However, burning of liquid fuel should be studied more thoroughly as the heat transfer process is very complicated.

(3) When carrying out dynamic correction on the flame height equation, the rotating flame height coefficient is expressed as $X_{fw} = \frac{u_z \Omega_z}{g}$. This coefficient reflects the burning and flow characteristics of fire whirl.

(4) Based on the earlier experimental results [8] and analysis in this paper with reference to literature, the boundary and initial conditions affect the motion of IFW and their effect is included in the factor α. Further investigation on α is required.

Acknowledgement

The work described in this paper was supported by a grant from the Research Grants Council of the Hong Kong Special Administrative Region, China for the project “A study of internal fire whirl in vertical shafts with open roofs” (PolyU 5137/13E) with account number B-Q37C.

References

[1] H.W. Emmons and S.J. Ying “The fire whirl” Eleventh Symposium (International) on Combustion, The Combustion Institute, Pittsburgh, Pennsylvanina, USA, p. 475-488 (1967).

[2] S. Soma and K. Saito “Reconstruction of fire whirls using scale models” Combustion and Flame, 86: 269-284 (1991).

[3] K. Satoh and K.T. Yang “Simulations of swirling fires controlled by channelled self-generated entrainment flows” Fire Safety Science - Proceedings of the Fifth International Symposium, p. 201-212 (1997).

[4] F. Battaglia, K.B. McGrattan, R.G. Rehm and H.R. Baum “Simulating fire whirls” Combustion Theory and Modelling, 4: 123-138 (2000).

[5] R.N. Meroney “Fire whirls, fire tornadoes and firestorms: Physical and numerical modelling” Proceedings of Physmod2003: International Workshop on Physcial Modelling of Flow and Dispersion Phenomena, 3-5 September 2003, Prato, Italy (2003).

[6] A.Yu. Snegirev, J.A. Marsden, J. Francis and G.M. Makhviladze “Numerical studies and experimental observations of whirling flames” International Journal of Heat and Mass Transfer, 47(12-13): 2523-2539 (2004).

[7] R.N. Meroney, “Fires in porous media: natural and urban canopies”, in: Ye.A. Gayev and J.C.R. Hunt (eds.), Flow and Transport Processes with Complex Obstructions, Springer, Chapter 8, p. 271-310 (2007).

[8] W.K. Chow, Z. He and Y. Gao, “Internal fire whirls in a vertical shaft”, Journal of Fire Sciences, 29: 71-92 (2011).

[9] FLUENT, http://www.ansys.com/products/fluid-dynamics/fluent/default.asp

[10] J.M. Chatris, J. Quintela, J. Folch, E. Planas, J. Arnaldos and J. Casal. “Experimental study of burning rate in hydrocarbon pool fires”, Combustion and Flame, 123(1-2): 1373-1383 (2001).

[11] A. Shinotake, S. Koda and K. Akita. “An experimental study of radiative properties of pool fires of an intermediate scale”, Combustion Science and Technology, 43(1-2): 85-97, (1985).

[12] B.J. McCaffrey, Purely Buoyant Diffusion Flames: Some Experimental Results, NBSIR 79-1910, National Institute of Standards and Technology, Gaithersburg, Maryland (1979).

[13] G. Heskestad “Engineering relations for fire plumes” Fire Safety Journal, 7(1): 25-32 (1984).

[14] Y. Hasemi and T. Tokunaga, “Flame geometry effects on the buoyant plumes from turbulent diffusion flames” Fire Science and Technology 4(1): 15-26 (1984).

[15] F.R. Steward “Prediction of the height of turbulent buoyant flames” Combustion Science and Technology, 2: 203 (1970).

[16] Y. Hayashi, K. Kuwana and R. Dobashi “Influence of vortex structure on fire whirl behavior” Fire Safety Science - Proceedings of the Tenth International Symposium, pp. 671-680 (2011).

[17] A.Y. Klimenko and F.A. Williams “On the flame length in fire whirls with strong vorticity” Combustion and Flame, 160: 335-339 (2013).

[18] K.H. Chuah and G. Kushida “The prediction of flame heights and flame shapes of small fire whirls” Proceedings of the Combustion Institute 31: 2599-2606 (2007).

[19] P.G. Saffman, Vortex Dynamics, New York: Cambridge University Press, pp. 11-30 (1992).

[20] N.A. Chigier, and J. M. Beer “Velocity and static pressure distributions in swirling air jets issuing from annular and divergent nozzles” Journal of Basic Engineering, 86: 788-796 (1964).

[21] V.I. Blinov, and, G.N. Khudiakov, Diffusion Burning of Liquids, U.S. Army Translation. NTIS No. AD296762 (1961).

[22] H.C. Hottel “Review certain laws governing diffusive burning of liquids, by V. I. Blinov and G. N. Khudiakov” Fire Research Abstracts and Reviews, 1: 41-44 (1958).

[23] J. Lei, N. Liu, L. Zhang, H. Chen, L. Shu, P. Chen, Z. Deng, J. Zhu, K. Satoh and J.L. de Ris “Experimental research on combustion dynamics of medium-scale fire whirl” Proceedings of the Combustion Institute, 33: 2407-2415 (2011).

[24] C.S. Tarifa, Open Fires, Instituto Nacional de Tecnica Aerospacial Esteban Teradas, Madrid (1967).

[25] H.C. Kung and P. Stavrianidis “Buoyant plumes of large-scale pool fires” Proceedings of the Combustion Institute, 19: 905-912 (1982).

[26] M.E. Klassen and J.P. Gore, Structure and Radiation Properties of Pool Fires, Final Report, in: NIST GCR 94-651, National Institute of Standards and Technology, Gaithersburg, MD (1994).

[27] K. Zhou, N. Liu, J.S. Lozano, Y. Shan, B. Yao and K. Satoh, “Effect of flow circulation on combustion dynamics of fire whirl”, Proceedings of the Combustion Institute 34: 2617-2624 (2013).

[28] J. Lei, N. Liu, L. Zhang, Z. Deng, N.K. Akafuah, T. Li, K. Saito and K. Satoh, “Burning rates of liquid fuels in fire whirls”, Combustion and Flame 159: 2104-2114 (2012).

[29] H. Koseki, “Combustion of large liquid pool fires”, Fire Technology 25(3): 241-255 (1989).